# Developing a 3 GHz HTS rf pulse compressor: Background

# High accelerating gradient

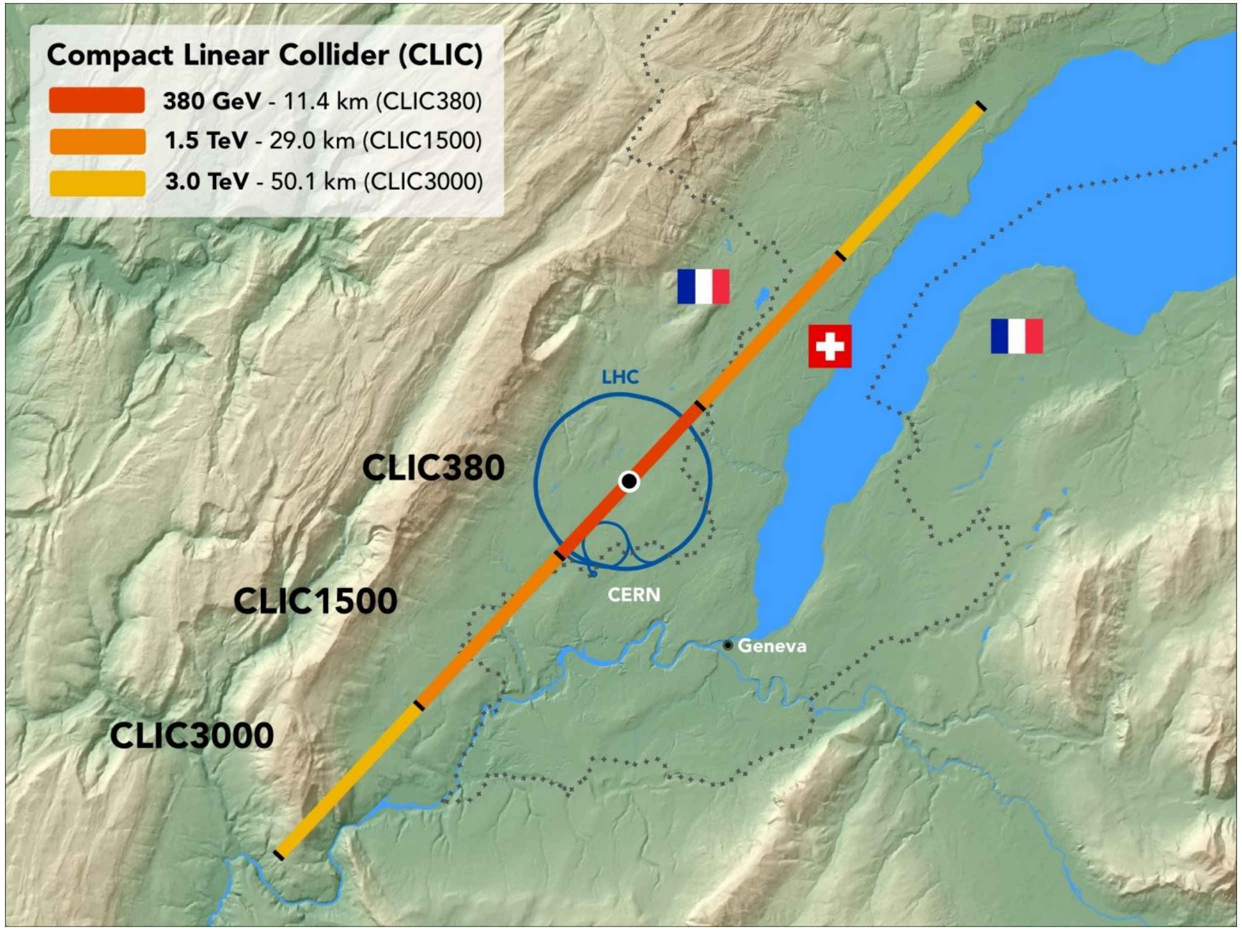

# Normal Conducting High Gradient

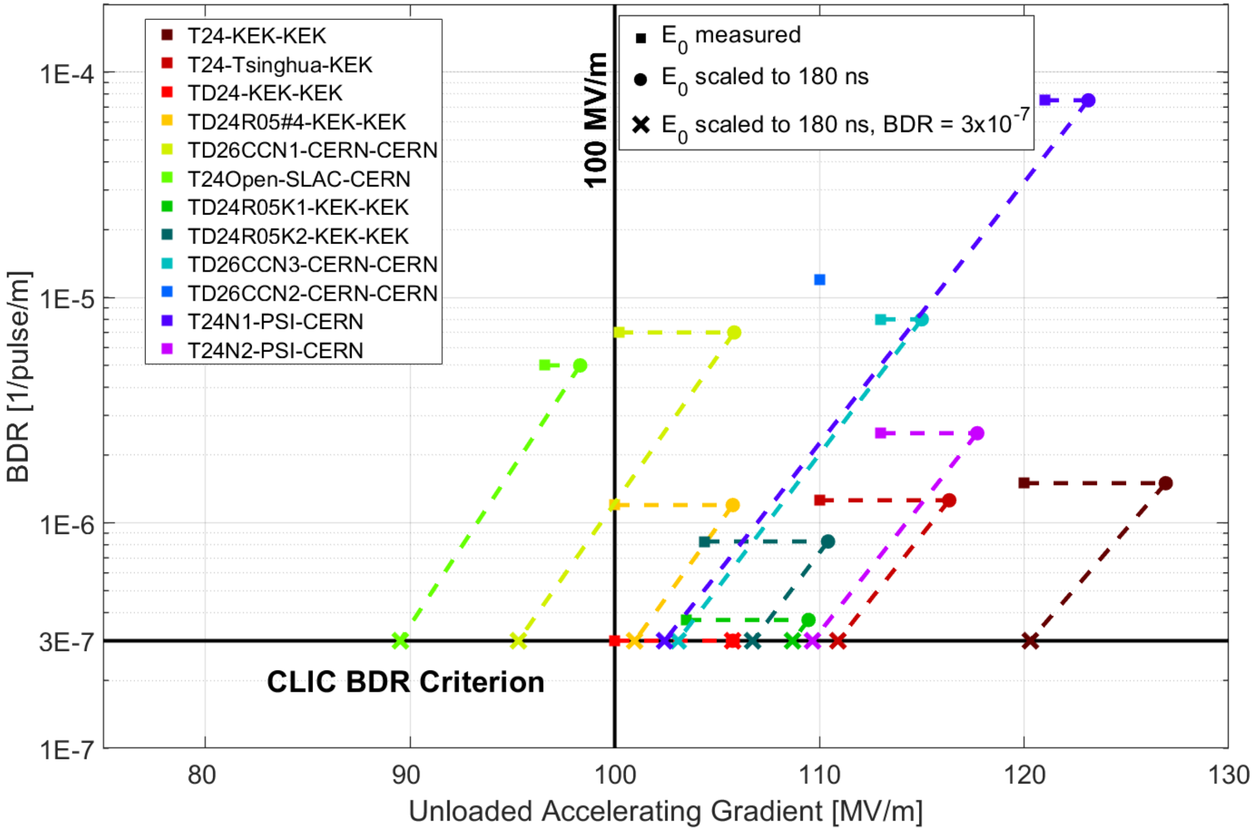


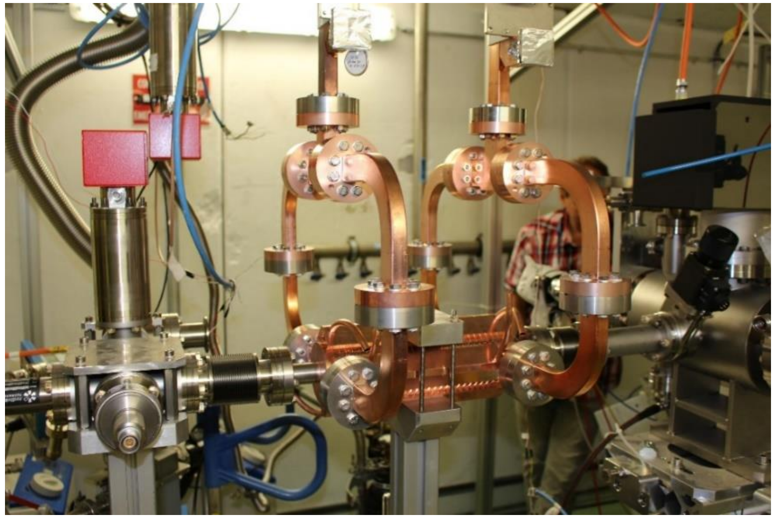

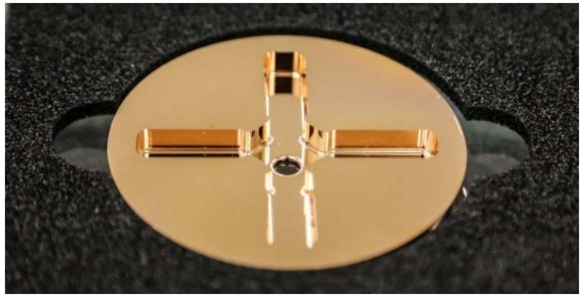

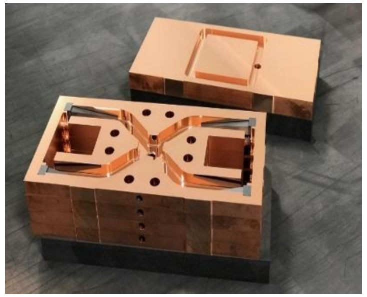

Peak surface electric fields about x 2.5 higher

https://doi.org/10.1103/PhysRevAccelBeams.21.061001,
https://doi.org/10.1103/PhysRevAccelBeams.20.052001 etc.

# Here in Valencia!

Contents lists available at ScienceDirect

Nuclear Engineering and Technology

journal homepage: www.elsevier.com/locate/net

Original Article

## High-power performance studies of an S-band high-gradient accelerating cavity for medical applications☆

P. Martinez-Reviriego [a,*], N. Fuster-Martínez [a,*], D. Esperante [a,b], M. Boronat [a], B. Gimeno [a], C. Blanch [a], D. González-Iglesias [a], P. Martín-Luna [a], E. Martínez [a], A. Menendez [a,b], L. Pedraza [a], J. Fernández [a], J. Fuster [a], A. Grudiev [c], N. Catalan Lasheras [c], W. Wuensch [c]

[a] Instituto de Fisica Corpuscular (CSIC-University of Valencia), Carrer del Catedrátic José Beltrán Martinez, 2, Paterna, 46980, Valencia, Spain
[b] Electronics Engineering Department, University of Valencia, Avinguda de l'Universita, Burjassot, 46100, Valencia, Spain
[c] CERN, Esplanade des particules, 1, Meyrin, 1211, Switzerland

ARTICLE INFO

*Keywords:*
High-gradient RF cavities
Linac
Hadron therapy

ABSTRACT

High-Gradient accelerating cavities are one of the main research lines in the development of compact linear accelerators. However, the operation of such accelerating cavities is currently limited by non-linear electromagnetic effects that are intensified at high electric fields, such as RF breakdowns, dark currents and radiation. A novel normal-conducting High Gradient S-band Backward Travelling Wave accelerating cavity for medical application (v = 0.38c) has been designed and constructed at CERN with a design gradient of 50 MV/m. In this paper, the high-power performance studies of this novel design carried out at the IFIC high-power laboratory are presented, as well as the analysis of the conditioning parameters in combination with numerical simulations.

*P. Martinez-Reviriego et al.*

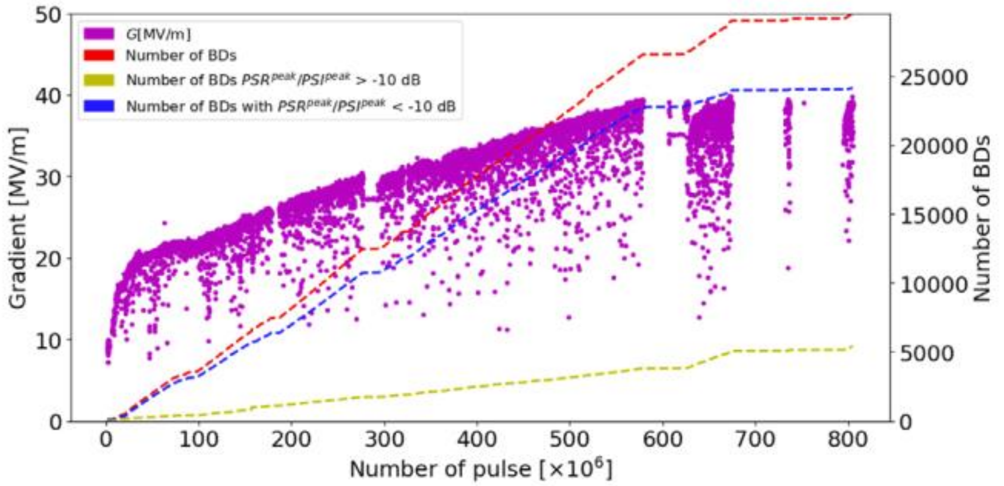


**Fig. 5.** History plot of gradient and cumulative number of BDs. (For interpretation of the references to colour in this figure legend, the reader is referred to the web version of this article.)

# Even higher-gradient through cooling to cryogenic temperatures

# Cryogenic copper - RF

**High gradient experiments with *X*-band cryogenic copper accelerating cavities**

A. D. Cahill* and J. B. Rosenzweig
*UCLA Los Angeles, California 90095, USA*

V. A. Dolgashev, S. G. Tantawi, and S. Weathersby
*SLAC Menlo Park, California 94025, USA*

(Received 14 December 2017; published 23 October 2018)

Vacuum radio-frequency (rf) breakdown is one of the major factors that limit operating accelerating gradients in rf particle accelerators. The occurrence of rf breakdowns was shown to be probabilistic, and can be characterized by a breakdown rate. Experiments with hard copper cavities showed that harder materials can reach larger accelerating gradients for the same breakdown rate. We study the effect of cavity material on rf breakdowns with short *X*-band standing wave accelerating structures. Here we report results from tests of a structure at cryogenic temperatures. At gradients greater than 150 MV/m we observed a degradation in the intrinsic cavity quality factor, $Q_0$. This decrease in $Q_0$ is consistent with rf power being absorbed by field emission currents, and is accounted for in the determination of accelerating gradients. The structure was conditioned up to an accelerating gradient of 250 MV/m at 45 K with $10^8$ rf pulses and a breakdown rate of $2 \times 10^{-4}$/pulse/m. For this breakdown rate, the cryogenic structure has the largest reported accelerating gradient. This improved performance over room temperatures structures supports the hypothesis that breakdown rate can be reduced by immobilizing crystal defects and decreasing thermally induced stresses.

https://doi.org/10.1103/PhysRevAccelBeams.21.102002

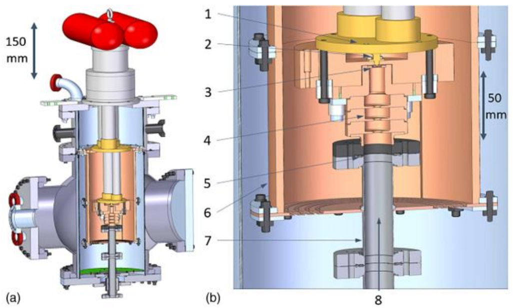


FIG. 3. (a) Solid model of the cryostat and (b) zoom in on Cryo-Cu-SLAC-#2 in same model. (1) Cold head of cryocooler; (2) current monitor; (3) brazed metal foil; (4) Cryo-Cu-SLAC-#2; (5) rf flange; (6) thermal shield; (7) Cu-plated stainless steel waveguide; (8) rf input.

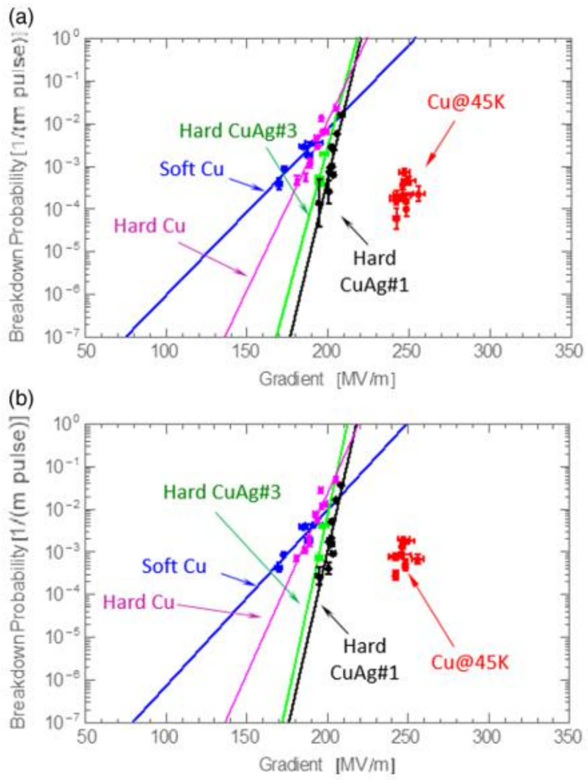


FIG. 11. Breakdown rate vs gradient:(a): first, trigger rf breakdowns; (b): all rf breakdowns. For the breakdown probability ~$10^{-4}$/pulse/m cryogenic structure clearly outperforms record data from hard CuAg [36].

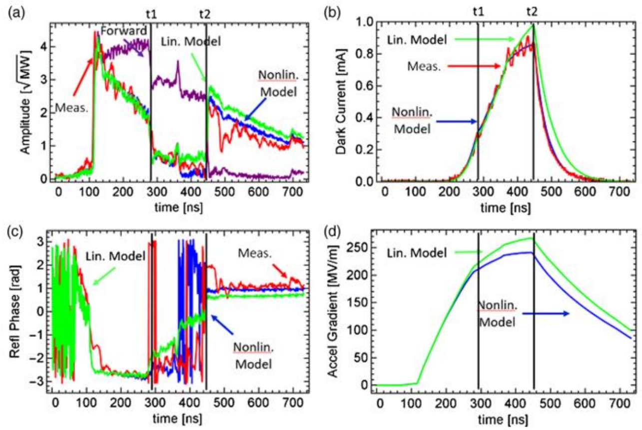


FIG. 6. Measured and reconstructed rf and current monitor signals for an example rf pulse. The measured current will be a small percentage of the field emitted current inside the cavity, which we estimated to be on the order of .1–1% [70]. Measured signals are in purple and red. Results of the nonlinear model are in blue and results from a linear model are in green. $t_1$ and $t_2$ are defined as the section where the input rf power is decreased to a lower power level and the gradient is flat, which for this pulse is 150 ns long.

VOLUME 90, NUMBER 22 PHYSICAL REVIEW LETTERS week ending 6 JUNE 2003

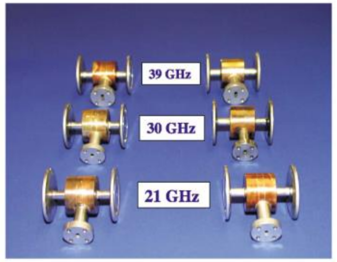


FIG. 2 (color online). Photograph of the six single cell cavities tested.

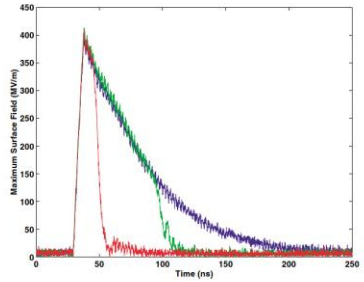


FIG. 3 (color online). Envelope of typical rf pulses with and without pulse shortening from a 30 GHz cavity.

https://doi.org/10.1103/PhysRevLett.90.224801

# Cryogenic copper – Pulsed dc

**Temperature-Dependent Field Emission and Breakdown Measurements Using a Pulsed High-Voltage Cryosystem**

Marek Jacewicz,[1,*] Johan Eriksson,[1] Roger Ruber,[1] Sergio Calatroni,[2] Iaroslava Profatilova,[2] and Walter Wuensch[2]

[1] *Department of Physics and Astronomy, Uppsala University, Regementsv. 1, 75237 Uppsala, Sweden*
[2] *CERN, European Organization for Nuclear Research, CH-1211 Geneva 23, Switzerland*

(Received 1 July 2020; revised 16 September 2020; accepted 3 December 2020; published 30 December 2020)

A variable-temperature pulsed high-voltage system has been constructed and a series of high-field measurements on copper electrodes have been carried out. The measurements are made at ambient to cryogenic temperatures and include conditioning, breakdown threshold, and field emission. A significant, up to 50%, increase in the breakdown threshold and remarkable stability of field emission are observed when cooled to cryogenic temperatures compared to room temperature. These results provide important experimental input for the development of quantitative theories and models of high-field processes as well as practical input for cryogenic radio-frequency systems.

https://doi.org/10.1103/PhysRevApplied.14.061002

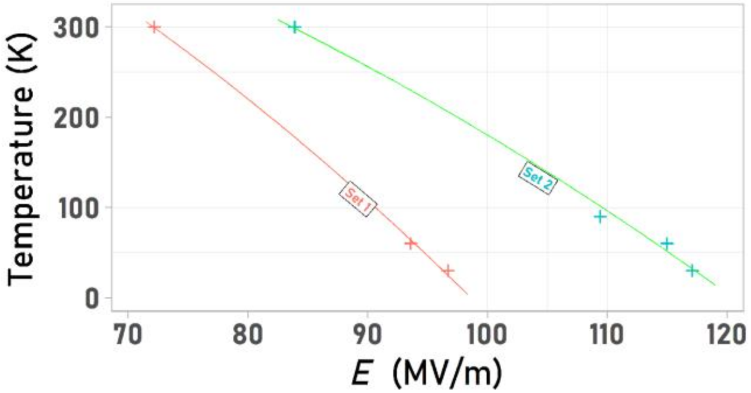


FIG. 2. Measured values of the maximum surface field at different temperatures for both sets of electrodes. The lines are the fits from the crystal defect model [Eq. (2)].

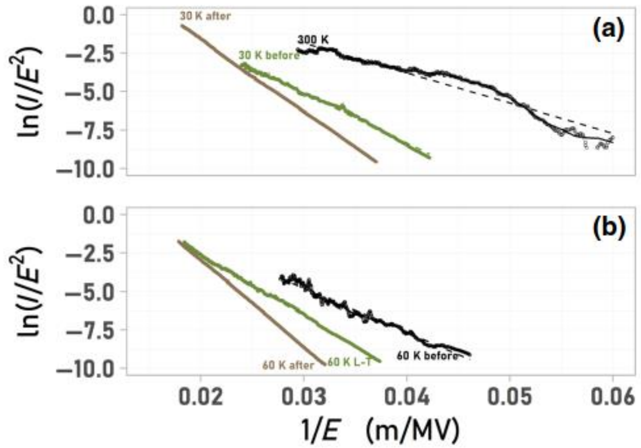


FIG. 3. (a) Field emission after conditioning at 300 K (black), cool-down to 30 K (green), and after re-conditioning at 30 K (brown). (b) FE for surface cooled down to 60 K after conditioning at 300 K (black), after re-conditioning at 60 K (brown), and compared with FE at 60 K after 9 days (green).

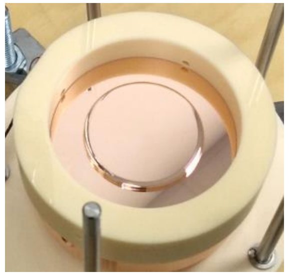

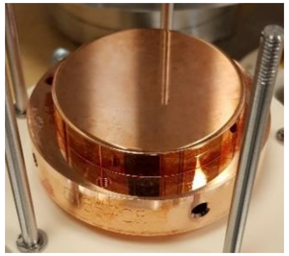

# Breakdown rate – Vacancy model

PHYSICAL REVIEW SPECIAL TOPICS - ACCELERATORS AND BEAMS **15**, 071002 (2012)

**Defect model for the dependence of breakdown rate on external electric fields**

K. Nordlund and F. Djurabekova

*Helsinki Institute of Physics and Department of Physics, University of Helsinki, P.O. Box 43, FIN-00014, Helsinki, Finland*

(Received 1 August 2011; revised manuscript received 2 April 2012; published 11 July 2012)

We develop an analytical model for the vacuum electric breakdown rate dependence on an external electric field, observed in test components for the compact linear collider concept. The model is based on a thermodynamic consideration of the effect of an external electric field on the formation enthalpy of defects. Although strictly speaking only valid for electric fields, the model also reproduces very well the breakdown rate of a wide range of radio-frequency breakdown experimental data. We further show that the fitting parameter in the model can be interpreted to be the relaxation volume of dislocation loops in materials. The values obtained for the volume are consistent with dislocation loops with radii of a few tens of nanometers.

https://doi.org/10.1103/PhysRevSTAB.15.071002

$$BDR \propto e^{\frac{-E^f + \varepsilon_0 E^2 \Delta V}{k_b T}}$$

$$E^f = 0.8\ eV$$

$$\Delta V = 0.8 \times 10^{-24} m^3$$

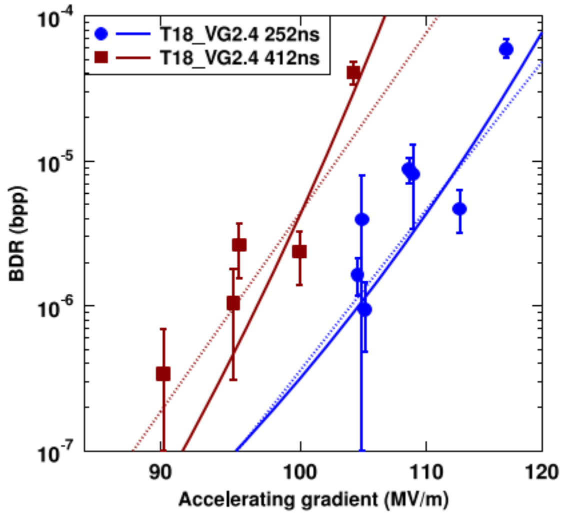


FIG. 4. Measured dependences of $R_{BD}$ (in units of breakdown per pulse, bpp) versus electric field for the T18 accelerating structure [33,43] and fits of our model (solid lines) as well as power laws (dashed lines) to the data.

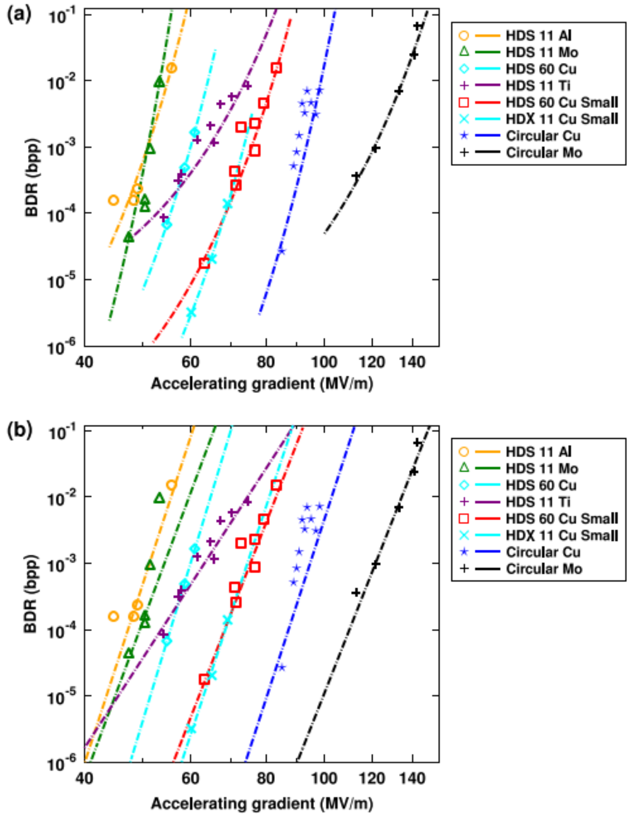


FIG. 3. (a) Measured dependences of $R_{BD}$ (in units of breakdown per pulse, bpp) versus electric field for different accelerating structures and fits of the model to the data. For clarity, the results of the functional fit are not shown for all $E$ values for all data sets. (b) Fits of power law functions to the same data. The experimental data and their labels are from [42].

# Breakdown rate – Dislocation dynamics model

PHYSICAL REVIEW LETTERS **120,** 124801 (2018)

### Stochastic Model of Breakdown Nucleation under Intense Electric Fields

Eliyahu Zvi Engelberg, Yinon Ashkenazy, and Michael Assaf
*Racah Institute of Physics and the Center for Nanoscience and Nanotechnology,*
*Hebrew University of Jerusalem, Jerusalem 9190401, Israel*

(Received 31 August 2017; published 20 March 2018)

A plastic response due to dislocation activity under intense electric fields is proposed as a source of breakdown. A model is formulated based on stochastic multiplication and arrest under the stress generated by the field. A critical transition in the dislocation population is suggested as the cause of protrusion formation leading to subsequent arcing. The model is studied using Monte Carlo simulations and theoretical analysis, yielding a simplified dependence of the breakdown rates on the electric field. These agree with experimental observations of field and temperature breakdown dependencies.

https://doi.org/10.1103/PhysRevLett.120.124801

Describing mobile dislocation population evolution:

$$\dot{\rho}^{+} = \frac{25\kappa C_t}{G^2 b}(\rho + c)\sigma^2 e^{-\frac{E_a - \Omega\sigma}{k_B T}}$$

$$\dot{\rho}^{-} = \frac{50\xi C_t}{G}\sigma\rho(c + \rho)$$

$$\sigma = \beta\epsilon_0 E^2/2 + ZGb\rho$$

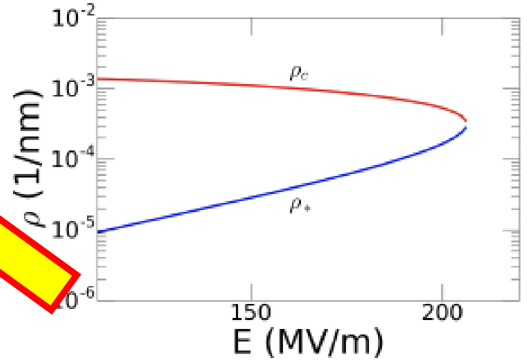


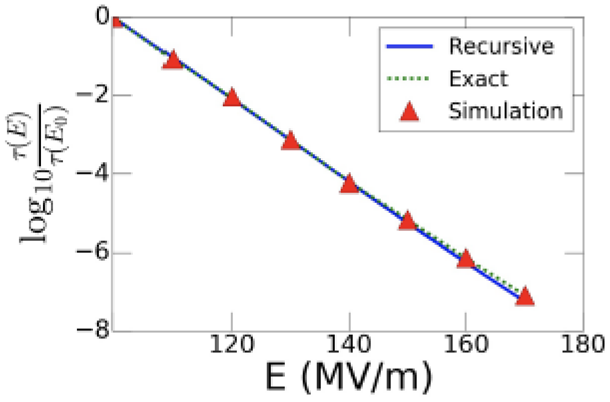


$$\tau \sim e^{-\gamma\frac{E}{E_0}}$$

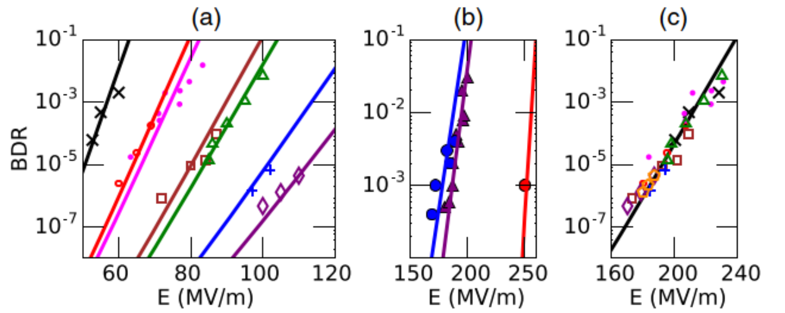


FIG. 3. Experimental BDRs with fitted theoretical lines using Eq. (7): (a) BDR versus $E$ for various Cu accelerating structures [11]. (b) BDR variation with $E$ at room temperature (two lines on the left) and at 45 K (line on the right) [51]. (c) BDR versus $E$ for various Cu accelerating structures [11,52], with $E$ rescaled so that all measurements are fitted with $\beta = 4.8$.

# $C^3$ – Cool Copper Collider

## $C^3$ Run plans

arXiv:2110.15800

- Planning for operations at high gradient: 120 MeV/m
  - Start at 70 MeV/m for C³-250
- Beam parameters optimized to record the same ILC luminosity within the same time frame and match physics goals

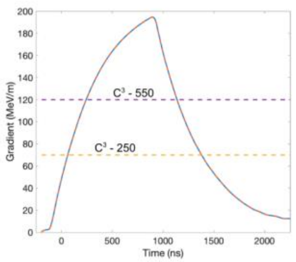


| Collider | $C^3$ | $C^3$ |
|---|---|---|
| CM Energy [GeV] | 250 | 550 |
| Luminosity [x10$^{34}$] | 1.3 | 2.4 |
| Gradient [MeV/m] | 70 | 120 |
| Effective Gradient [MeV/m] | 63 | 108 |
| Length [km] | 8 | 8 |
| Num. Bunches per Train | 133 | 75 |
| Train Rep. Rate [Hz] | 120 | 120 |
| Bunch Spacing [ns] | 5.26 | 3.5 |
| Bunch Charge [nC] | 1 | 1 |
| Crossing Angle [rad] | 0.014 | 0.014 |
| Site Power [MW] | ~150 | ~175 |
| Design Maturity | pre-CDR | pre-CDR |

9m module
8 structures
Up to 1 GeV acceleration

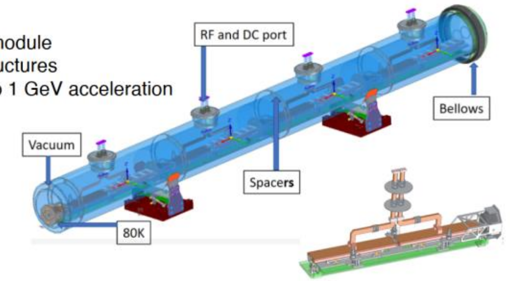


SLAC Caterina Vernieri · C³ 2024 · February 12, 2024 6

## Introduction Staged Approach

- $C^3$ accelerator technology: Modularized linac based on liquid N2 cooled C-band cavity.
- Cryomodules (CM)s are vacuum insulated cryostats housing 4 rafts, and has 75 cm ID and about 9 m long.
- Rafts are mechanical supporting structures consisting of 2 accelerator structures and one quadrupole magnet. They are pre-aligned at 300K to 5 microns. Each raft has mechanical actuators to align one raft to the next with 5 degrees of freedom.

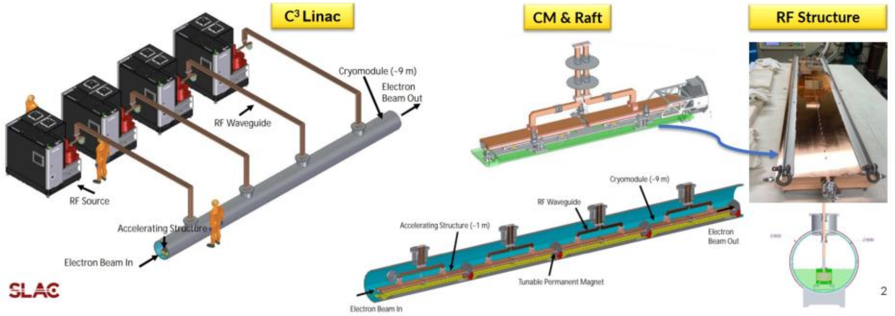


2

## RF Parameters – $C^3$250/550 GeV

- At $C^3$ the same LINAC can deliver 250 GeV c.o.m and 550 GeV c.o.m in 8 km
- The optimized structure can reach 300 MΩ/m at 80K.
- The accelerator beam aperture (diameter) is 5.2 mm.

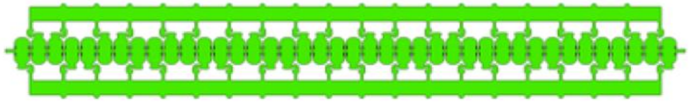

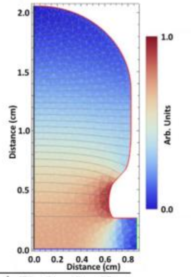


- Each CM can reach up to 0.7 GeV with 4 X 50MW klystrons .

| Gradient (MV/m) | Power diss. (W) | rf flat top (ns) | Pulse compr. | Comments | Power/area (W/cm$^2$) | $\Delta T$ Cu-bulk to LN$_2$ (K) |
|---|---|---|---|---|---|---|
| 70 | 2500 | 700 | N | $C^3$ -250 | 0.393 | 2.3 |
| 120 | 2500 | 250 | N | $C^3$ -550 | 0.393 | 2.3 |
| 155 | 3900 | 250 | N | $C^3$ -550 in 7 km | 0.614 | 2.5 |
| 120 | 1650 | 250 | Y | $C^3$ -550 | 0.259 | 2.1 |

SLAC Ref: E. Nanni et al, SLAC-PUB-17660 3

Person view:

- Advantage – Lower peak power requirement, fewer power sources.
- Disadvantage – Lower efficiency. Limited increase in copper conductivity compared to Carnot cooling cost.
- Challenge – Micron-level alignment in LN2 environment.

# RF pulse compressors

RF pulse compressors are high $Q$ cavities that can store and quickly discharge RF energy, giving a power gain. High $Q_0$ is crucial for this application, usually around 200,000.

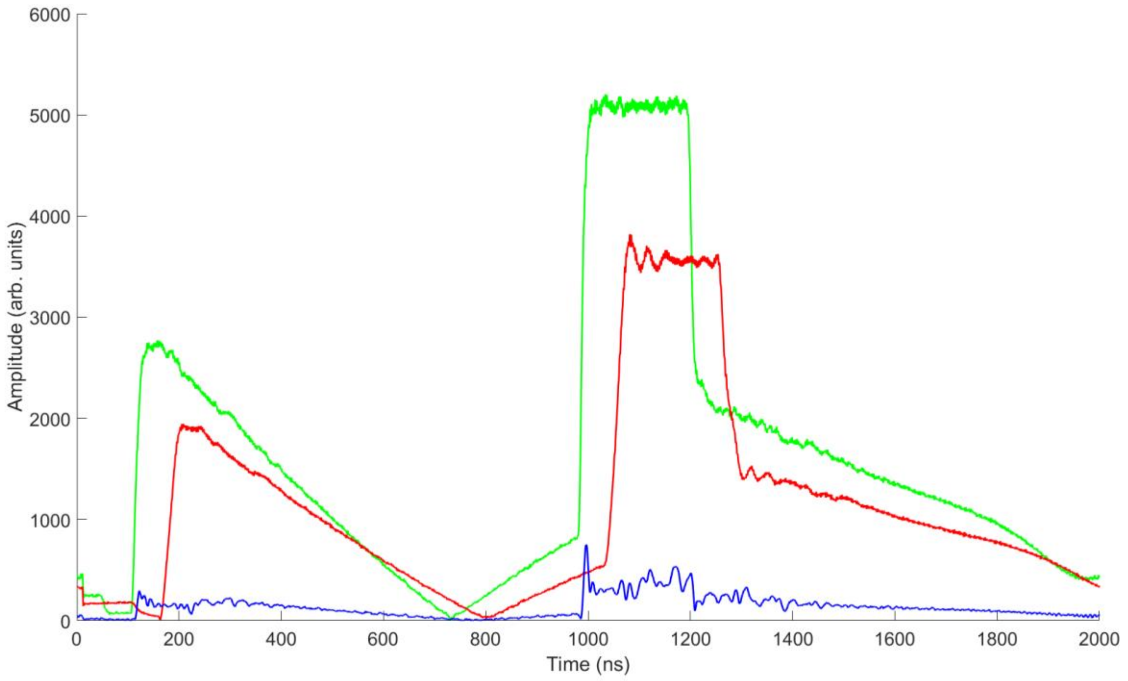


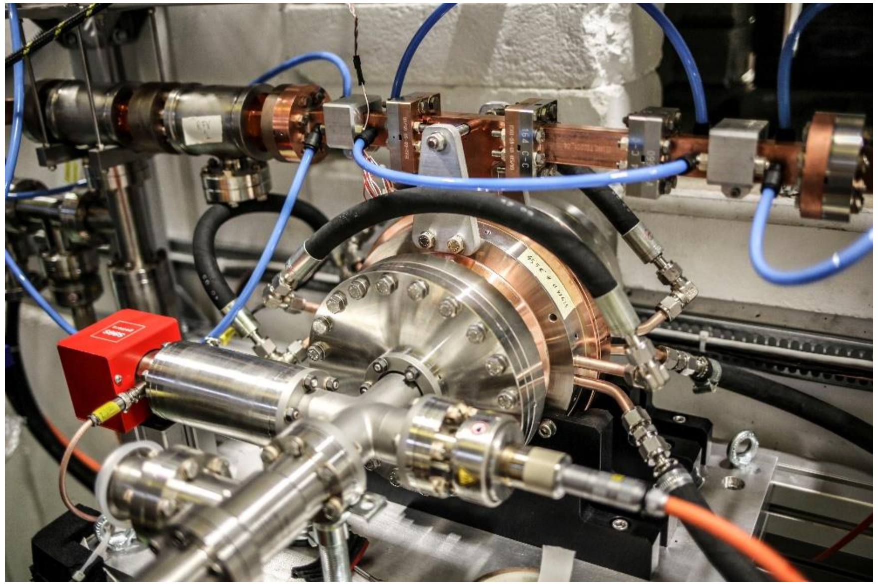

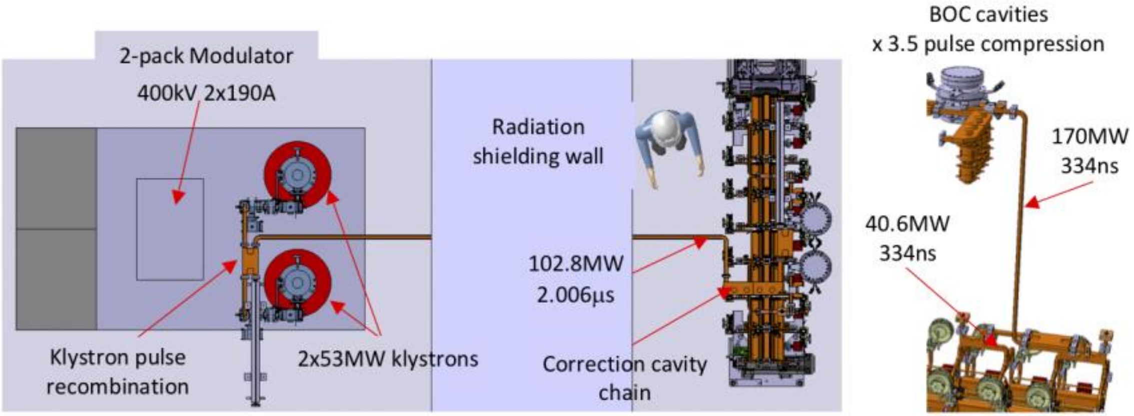


**Figure 3.2:** The RF unit: top view of one RF unit in the klystron and Main-Linac tunnels (left) and detailed view of the distribution network (right).

# Accelerator Outlook: Pulse Compressor

Pulse compressor tests (11.4 GHz) with HTS tape at SLAC  coming soon

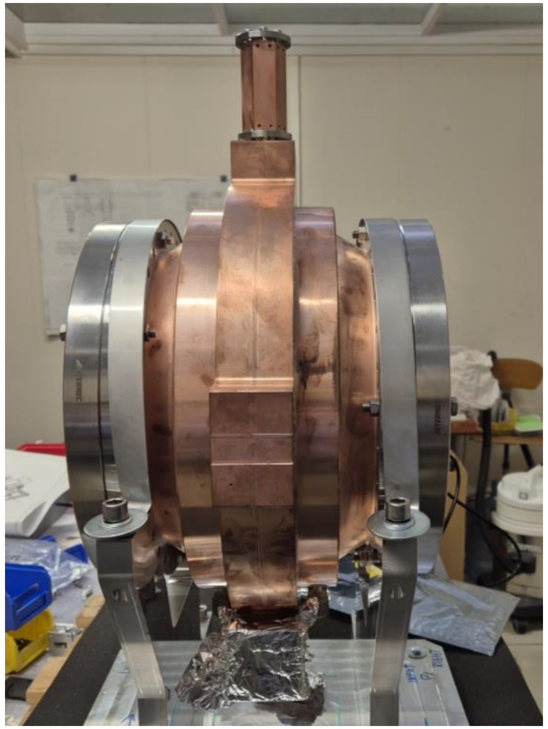

Photo by Ankur Dhar

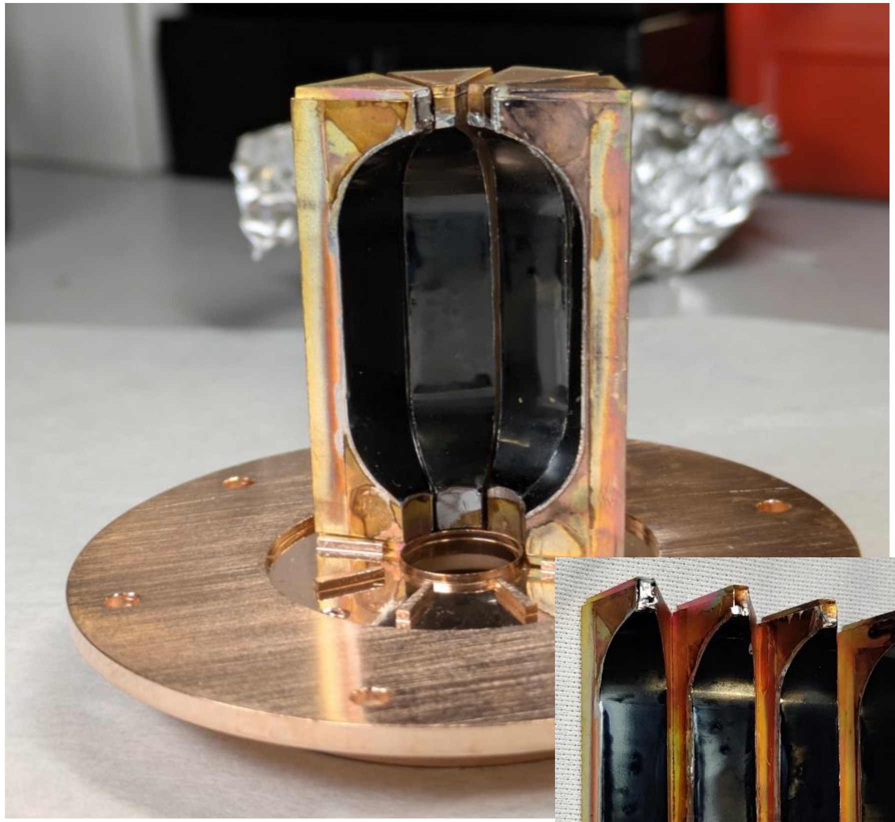

G.Le Sage

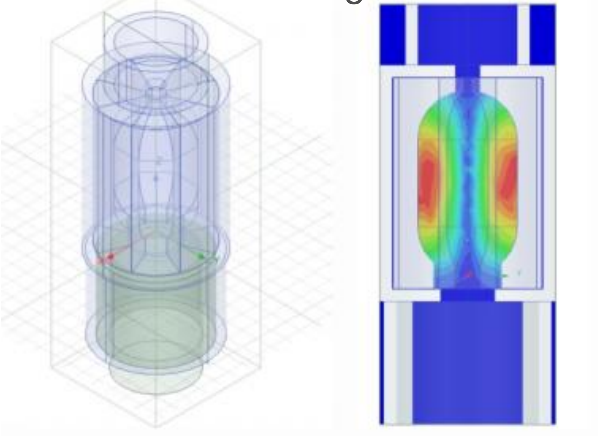

Octagonal cavity exciting the TM010 mode was designed. This allows currents to run longitudinally.

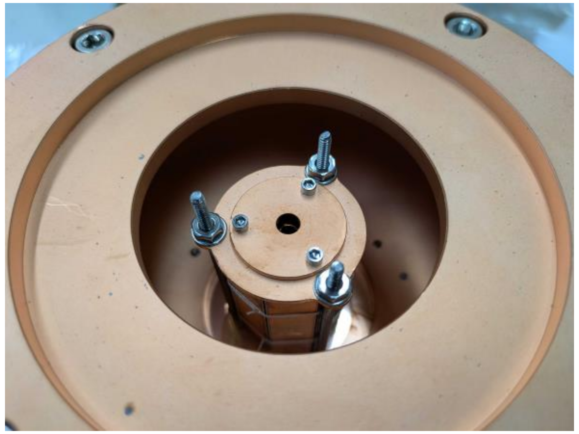

# Axion haloscope cavities and high quality factor from HTS

# Low temperature first

# Motivation and Cavity preparation

Motivation:

Axion haloscope

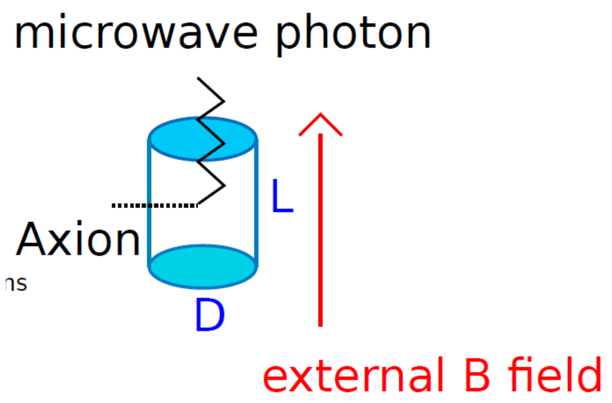


$$\mathcal{F} \sim g_{A\gamma}^{4}\, \boldsymbol{Q}\, T_{sys}^{-2} V^{2} G^{4} m_{A}^{2}\, \boldsymbol{B^{4}}$$

Increase Q
copper coating → superconducting coating

**Requirement:** High quality factor in a high external DC magnetic field

Tape attached at ICMAB by G. Telles, N. Lamas, X. Granados, T. Puig, J. Gutierrez

# Achievements

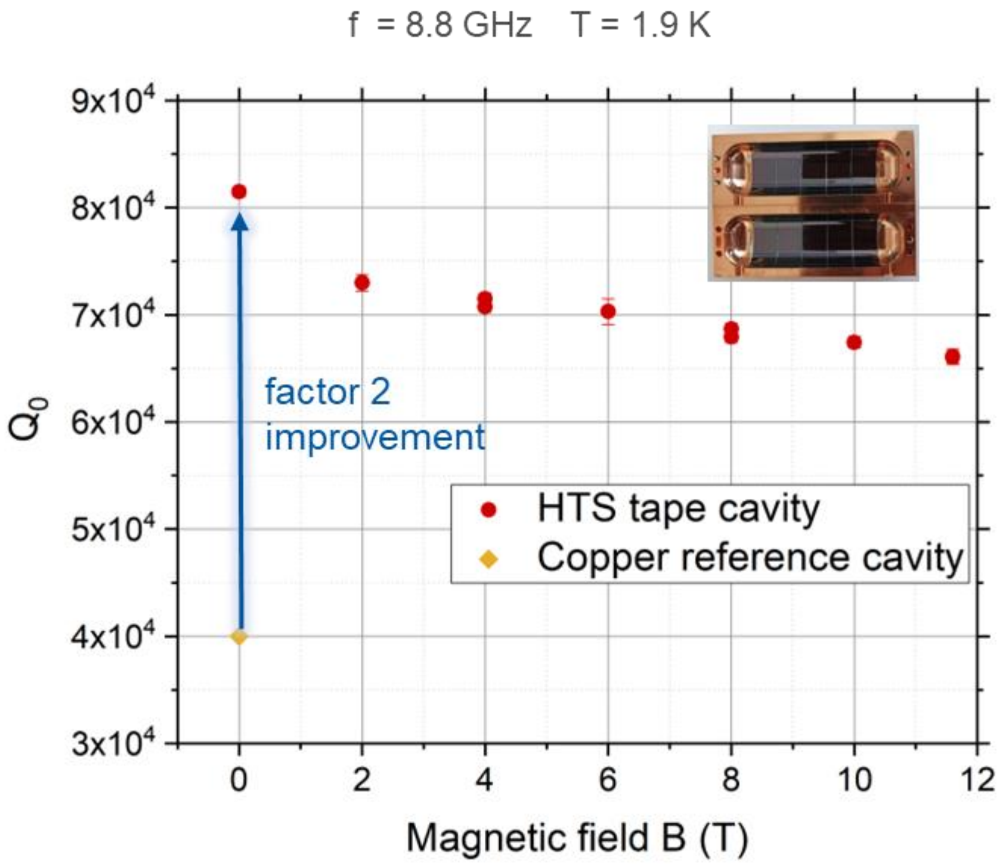


Factor of 20 improvement from room temperature Cu to 4 K HTS

Factor of 6 improvement from 4 K Cu to 4 K HTS

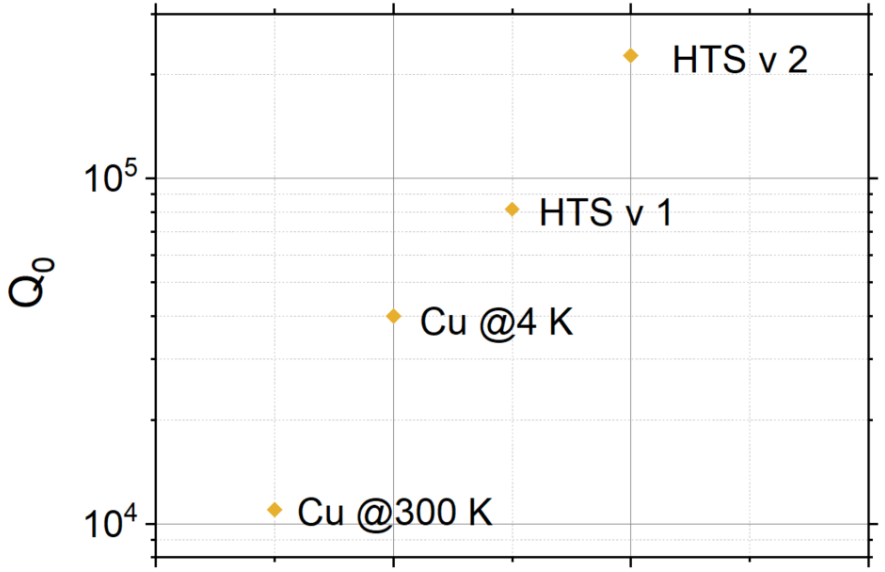


Coatings characterised without magnetic field @ 9 GHz on standardized RADES cavity

# Achievements from other Experiments

**CAPP Experiment: Q0 of 1.3 E7 achieved @ 5.4 GHz and at 8 T**

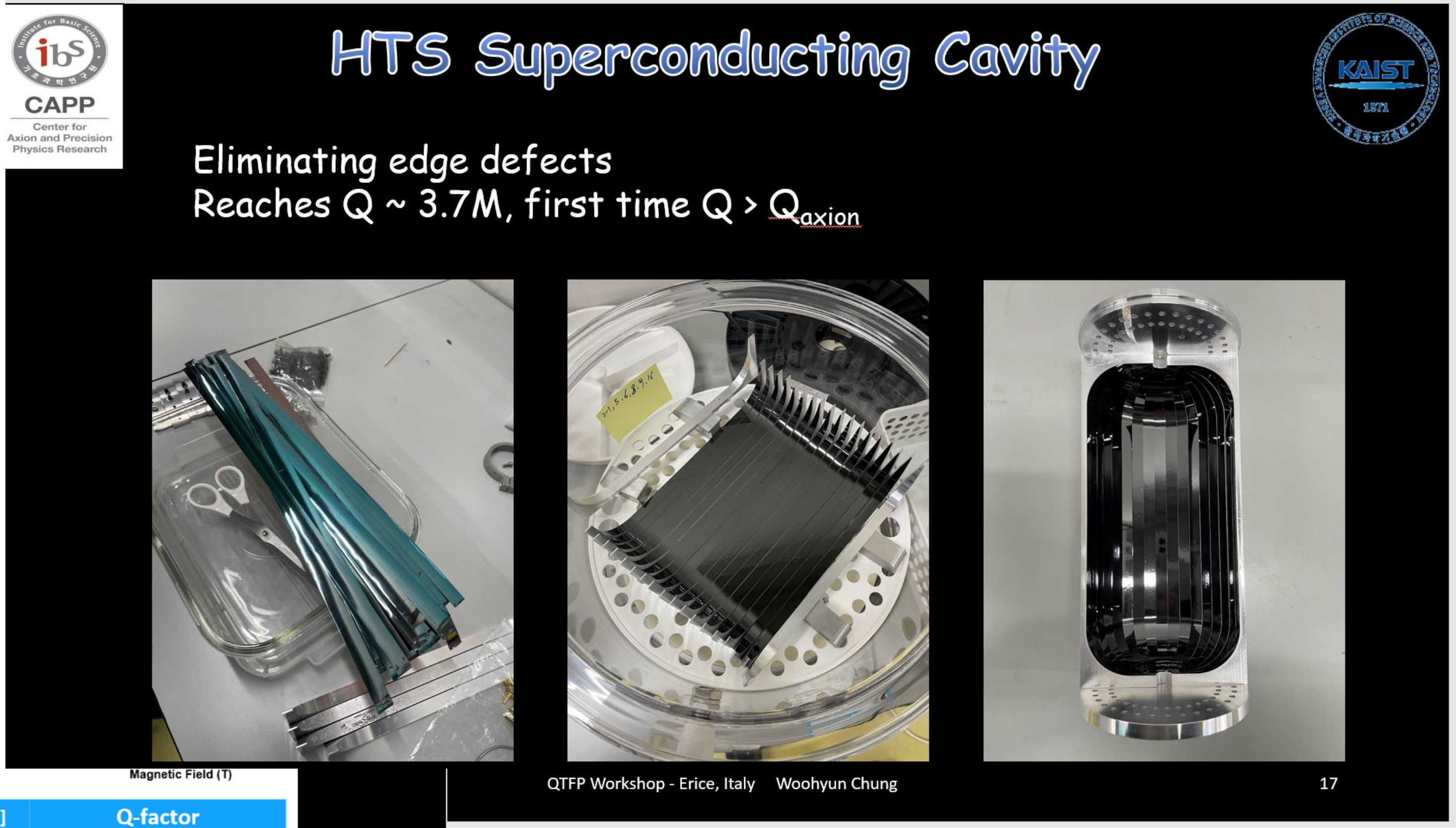


Differences to RADES:

- Geometric factor
- Almost no bending of tape
- Low frequency and $f^2$ scaling of Q

Magnetic Field (T) Magnetic Field (T) Magnetic Field (T)

| Generation | Material | Substrate | Volume [liters] | Frequency [GHz] | Q-factor |
|---|---|---|---|---|---|
| 1st Gen | YBCO | NiW | 0.3 | 6.9 | 150,000 @ 8 T |
| | | | | | 330,000 @ 8 T |
| 2nd Gen | GdBCO | Hastelloy | 1.5 | 2.3 | 500,000 @ 8 T |
| 3rd Gen | EuBCO + APC | Hastelloy | 0.2 | 5.4 | 13,000,000 @ 8 T |
| | EuBCO + APC | Hastelloy | 1.5 | 2.3 | 3,700,000 @ 8T |
| | EuBCO + APC | Hastelloy | 36 | ~ 1 | ? |

Sep. 3rd 2023 QTFP Workshop - Erice, Italy Woohyun Chung 19

# Outlook: HTS direct coating for axion detectors

**Layer architecture**

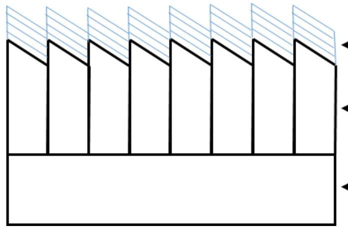


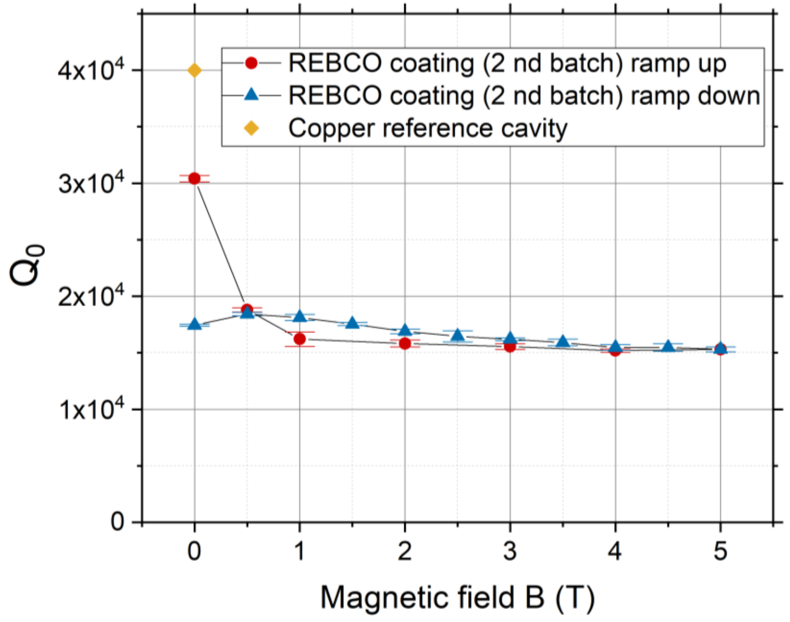


Coated by THEVA and Ceraco by EB- PVD

**ISD deposition**

- buffer layer is required , which provides a biaxially textured surface
- Deposition of MgO layer on an inclined substrate

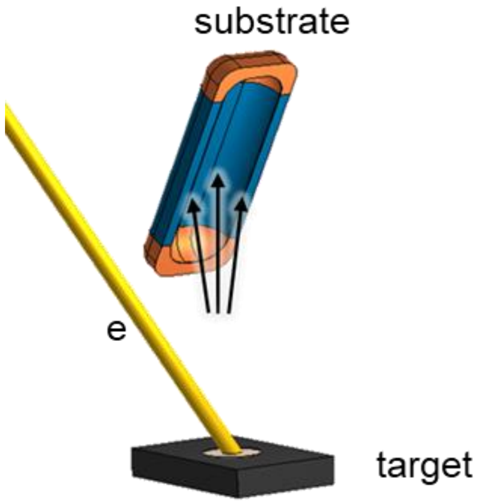


Cavity made of flat pieces would have been more advantageous for this coating

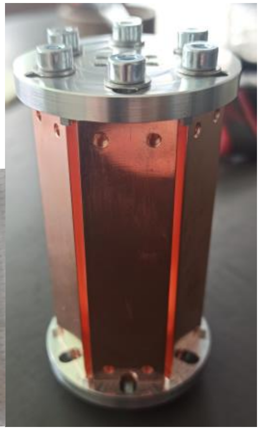

Now moving from low-power and low-temperature to high-temperature and high-power

# HTS high power characterisation test stand

Test stand at SLAC:

- High-Q X-band hemispheric cavity with a $TE_{032}$-like mode at 11.4 GHz.
- Zero E-field and maximum H-field on the sample
- Sample accounts for ⅓ of total cavity loss
- Can achieve $H_{peak}$ of about 360 mT using 50 MW XL-4 Klystron.

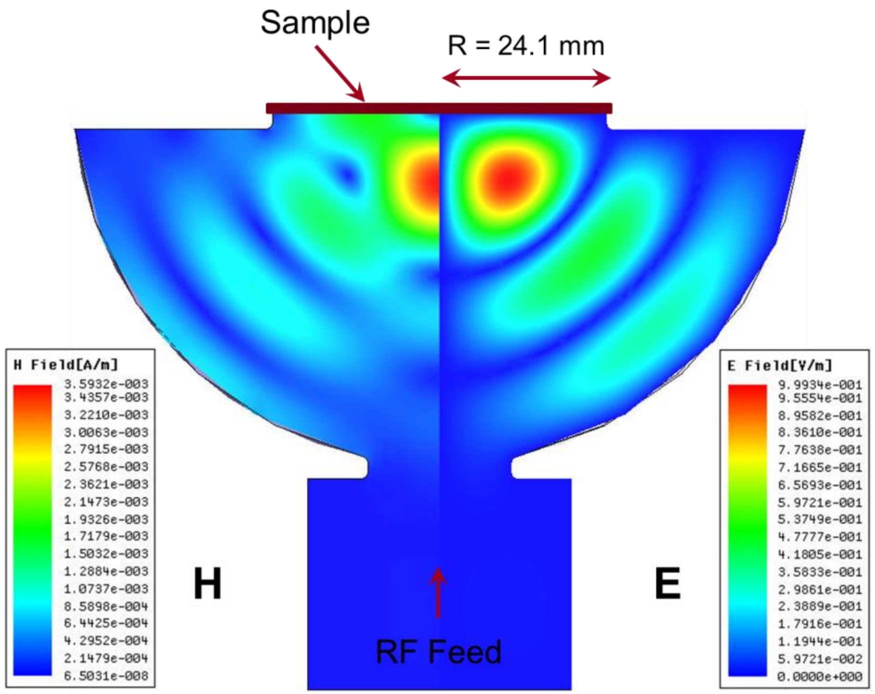


# HTS low power characterisation of flat samples

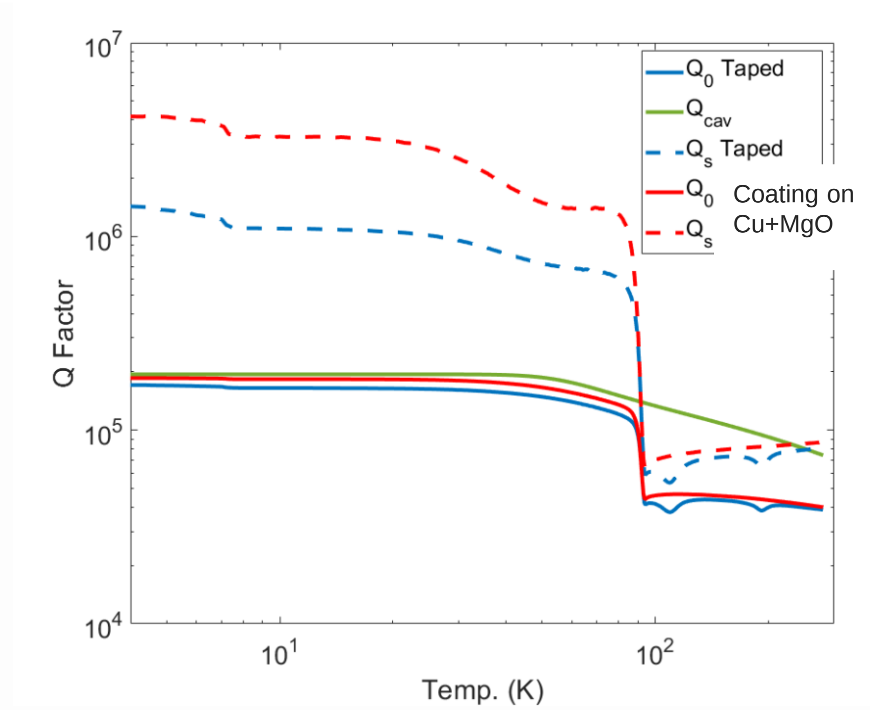


Experiment at SLAC, plots by:
E. Nanni
M. Schneider
A. Dhar

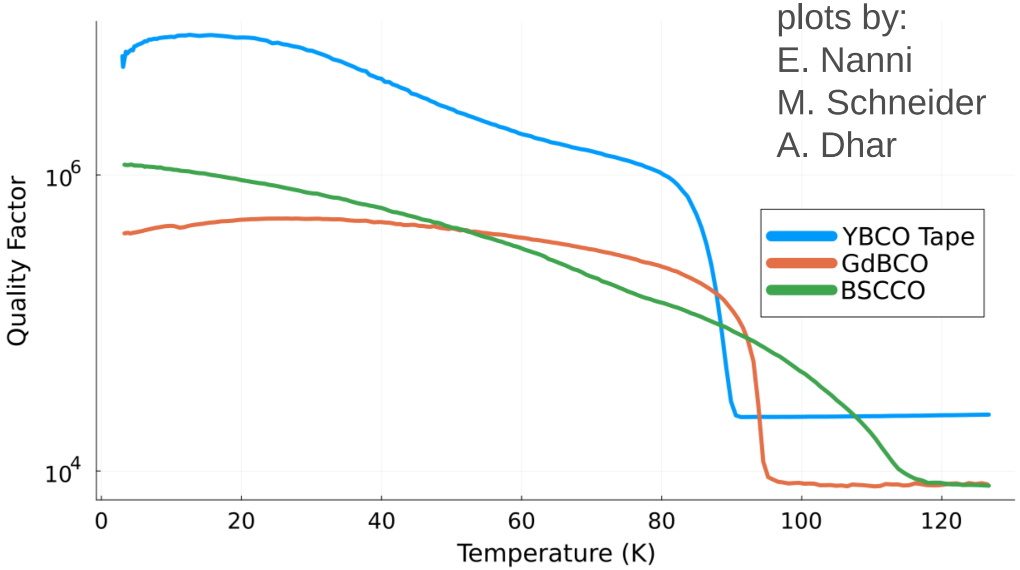


| Improvement compared to | (a) HTS tape | (b) HTS coating |
|---|---|---|
| Cu disc @ 4 K | 10 | 16 |
| Cu disc @ 80 K | 4 | 5 |

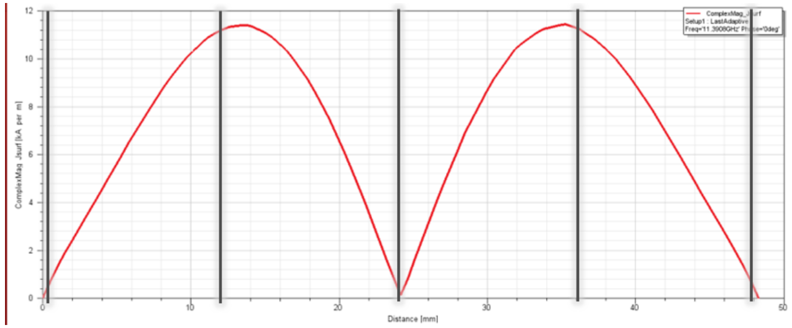

# Summary and Conclusion

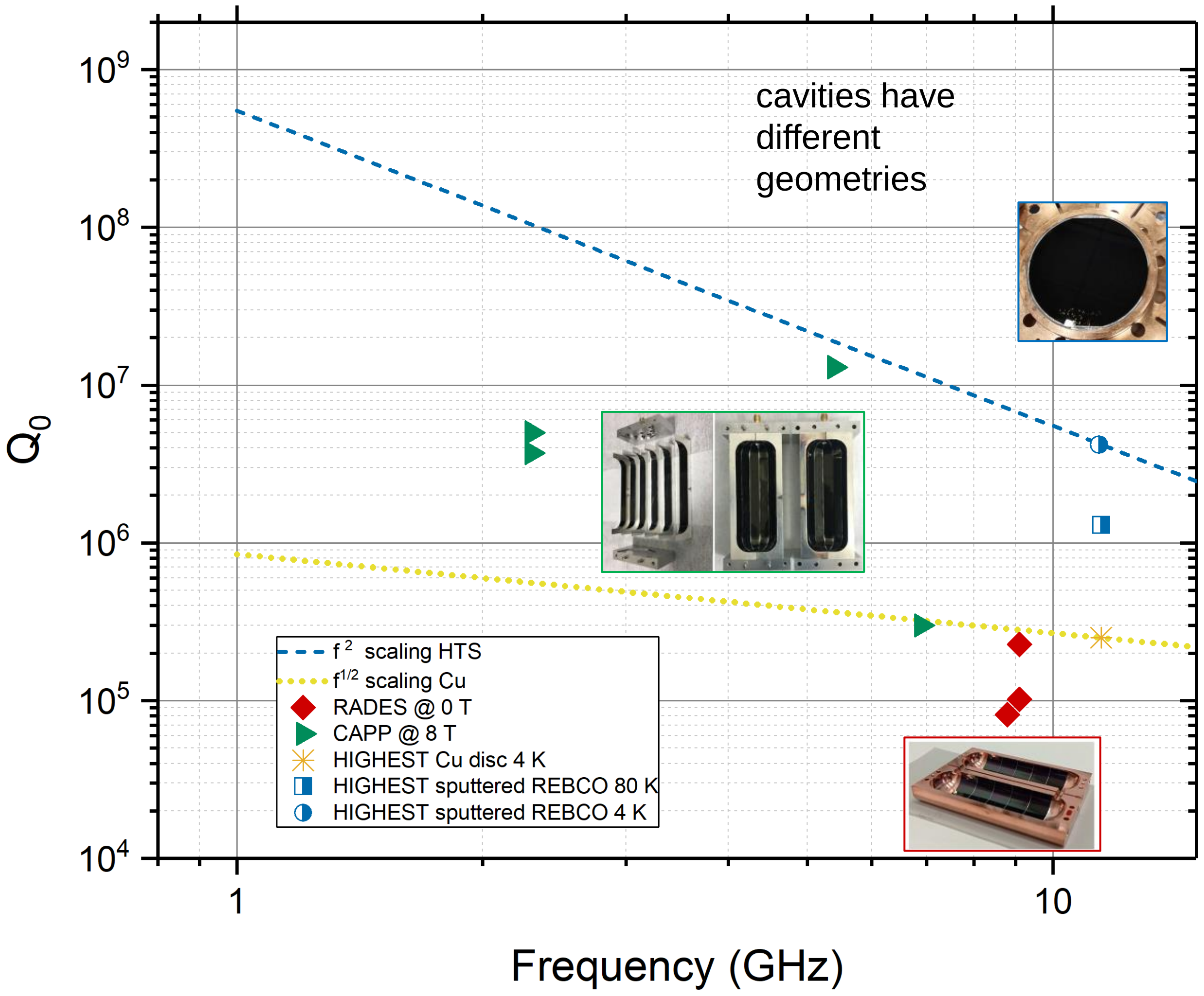


**Fig 1: Summary of low-power HTS characterisation results**

- High power RF use of HTS looks extremely promising
- So far no hints of performance limit in RF current up to the maximum power available in the test
- The next step is to go from TWT to a Klystron to see where the limits are

We have all the key scientific and technological elements to build a 3 GHz HTS pulse compressor!